JOURNAL OF Materials CHEMISTRY

Amorphous very high surface area silica macrostructures

Lubomira Tosheva,[a] Valentin Valtchev†[b] and Johan Sterte*[a]

[a]*Division of Chemical Technology, Luleå University of Technology, S-971 87 Luleå, Sweden. E-mail: jost@km.luth.se*
[b]*Laboratoire de Materiaux Mineraux, ENSCMu, Université de Haute Alsace, UPRES-A CNRS 7016, 3, rue Alfred Werner, 68093 Mulhouse Cedex, France*

Received 9th February 2000, Accepted 3rd July 2000
First published as an Advanced Article on the web 14th August 2000

A procedure for the preparation of amorphous silica spherical macroparticles using strongly basic anion exchange gel resins as shape directing macro-templates is presented. Resin beads were hydrothermally treated with either clear homogeneous TPA–silicate solutions containing tetraethoxysilane, tetrapropylammonium hydroxide and distilled water or with sodium silicate solutions. As a result of the ion exchange of silica species into the resin structure, resin–silicate composites were formed. After separation and drying of the resin–silicate composites, the resin was removed by combustion leaving solid spherical silica particles with surface areas exceeding 1000 $m^2 g^{-1}$. Two types of gel resins having different active groups and degrees of cross-linking were employed and the products obtained were characterised by SEM, Raman spectroscopy and nitrogen adsorption measurements. The type of the resin as well as the type of silicate solution used were of great importance for the pore structure of the final materials.

1 Introduction

In recent years, intense research has been dedicated to the fabrication of materials with predetermined shapes, *e.g.*, spherical. Applications for such materials cover a broad range of areas such as catalysis, coatings, composite materials and molecular sieving. Methods have been developed for producing a number of materials including ceramic oxides and glasses, metals, polymers and organic compounds in the form of spheres.[1] Often, the size of the spherical particles as well as their specific surface area, pore structure, mechanical and thermal properties are of great technological importance. Pore structures can be tailored using template-based approaches[2] where template describes a central structure about which a network forms in such a way that removal of the template creates cavities with morphological features related to the template.[3] Thus, microstructured porous silica has been obtained *via* polymerisation of silica solutions in the cavities of modified latex particles and subsequent removal of the colloidal crystal templates.[4] Latex particles have been used as templates for the preparation of hollow silica spheres with controlled wall thickness through the layer-by-layer (LbL) method, followed by removal of the templated core.[5]

The sol–gel method has been used to prepare millimetre-sized porous silica spheres.[6,7] Hollow as well as hard mesoporous silica spheres have been prepared through emulsion biphase chemistry.[8,9] Mesoporous silica spheres have also been synthesised under quiescent aqueous acidic conditions.[10] Monodispersed mesoporous MCM-41[11] and MCM-48[12] spheres have been synthesised by a modified Stöber[13] method.

Recently, a novel method for the preparation of zeolite spheres based on the use of macroporous anion exchange resins as shape directing macro-templates was reported.[14] In this method, zeolite crystallises in the pores of the resin and after the synthesis the resin is removed by combustion leaving self-bonded zeolite spheres. The present work reports on the synthesis of amorphous silica spheres employing TPA–silicate or sodium silicate solutions using gel resins as starting macro templates. Owing to the difference in structure between gel type resins and macroporous resins, materials with properties quite different from those of the ones prepared using macroporous resins were obtained. Macroporous resins have a permanent network of pores and high surface areas in the dry state whereas gel type resins are composed of a cross-linked infinite network of interpenetrating polymer chains without any fine structure and have very low surface areas in the dry state.[15] The influence of the type of gel resin and the solution composition on the properties of the final materials was investigated.

2 Experimental

2.1 Sample preparation

Two types of styrene–divinylbenzene strongly basic anion exchange gel resins (chloride ionic form) from Dowex, 1X2-100 and 2X8-100, were used in the experiments. The resins have ion exchange capacities of 0.7 and 1.2 meq ml^{-1}, respectively, and are supplied in the form of spherical particles with a dry mesh range of 50–100. Cross-linkage, as indicated in the resin designations, is 2% and 8%, respectively. Gel resins were mixed with TPA–silicate solutions in polyethylene reaction vessels and treated in a silicon oil bath preheated to 100 °C under reflux for 48 h. In a typical experiment 2 g of the ion exchanger were weighted in a polyethylene reactor and then 20 g of the corresponding TPA–silicate solution were added. Two TPA–silicate solutions were prepared by mixing tetraethoxysilane (TEOS) (Merck, >98%) with tetrapropylammonium hydroxide (TPAOH) (Merck, 20% aqueous solution) and distilled water followed by 12 h of hydrolysis.[16] The molar compositions of the solutions were 9 TPAOH : 25 SiO_2 : 480 H_2O : 100 EtOH (A) and 3 TPAOH : 25 SiO_2 : 404 H_2O : 100 EtOH (B). The presence of ethanol (EtOH) in these compositions is a consequence of the use of TEOS as a silica source.

In the absence of ion exchanger and under the conditions described (treatment at 100 °C for 48 h) solutions A and B yield silicalite-1.[16] The crystallisation process seems to be unaffected by the presence of macro-templates and silicalite-1 crystallises in the bulk phase of the syntheses. The silicalite-1 crystallised in the bulk has, however, not been studied in detail since the

†Also at Central Laboratory of Mineralogy and Crystallography, Bulgarian Academy of Sciences, Sofia, Bulgaria.

 DOI: 10.1039/b001096k

primary objective of the present study was to prepare solid macrostructures.

In another series of experiments, the resin particles were mixed with sodium silicate (water glass) (21.4 wt% SiO_2, 6.7 wt% Na_2O, Akzo Nobel, Sweden) (C) in a weight ratio of 1 : 10 and treated in an oil bath at 100 °C for different times. Initially, the resin beads were floating on the surface of the viscous water glass. After *ca.* 6 h of treatment the resin particles sank. This time of treatment (6 h) was used to prepare samples employing solutions A, B and C diluted 10 and 20 times (designated as A10, A20, *etc.*). The treatment with the diluted solutions was performed at 100 °C as well.

As a result of the treatment of the gel resins with the silicate solutions, resin–silicate composites were obtained. These composites were separated from the mother liquid (or from the silicalite-1 crystallised in the bulk when solutions A and B were used) by decanting, washed several times with distilled water and treated in a 0.1 M ammonia solution in an ultrasonic bath for 5 min. The particles were then washed again and dried at 60 °C. The organic macro-template was finally removed by calcination at 600 °C for 5 hours, after heating to this temperature at a rate of 1 °C min^{-1}.

2.2 Characterisation

A Philips XL 30 scanning electron microscope (SEM) equipped with a LaB_6 emission source was used for studies of the morphology of the samples. Raman analysis was performed with a Perkin-Elmer PE 1700X NIR FT-Raman spectrometer equipped with a Nd–YAG laser operating at 1064 nm. The spectra were collected at room temperature averaging 500 scans with a spectral resolution of 4 cm^{-1} using 1 W of the incident light. Before Raman analysis the spherical particles were ground into a powder. Specific surface areas were calculated with the BET equation using nitrogen adsorption data obtained with a Micromeritics ASAP 2010 surface area analyser. Samples were outgassed at 300 °C overnight prior to analysis. The total pore volume was obtained by converting the amount adsorbed at a relative pressure of 0.995 to the volume of liquid adsorbate. Pore-size distributions were determined by the BJH method (desorption isotherm).

3 Results and discussion

3.1 TPA–silicate solutions

SEM micrographs of the starting ion exchange resin beads (a), the resin–silicate composites obtained after 48 h treatment at 100 °C in the TPA–silicate solutions A and B (b) and the corresponding calcined particles (c) are shown in Fig. 1. As seen from this figure the resin–silicate composites were similar in size and shape to the original resin beads (Fig. 1a,b). However, upon calcination the particles seem to shrink slightly and also a certain number of particles tend to disintegrate (Fig. 1c). SEM was not found to be an appropriate technique to estimate the percentage of broken particles owing to difficulties in preparing representative samples and no general conclusions can be drawn either for this number or for the influence of the resin type or the solution type on the mechanical stability of the particles. The disintegration of the particles may occur during: (i) drying when the swelled resin–composite particles shrink or (ii) calcination when a considerable amount of organic matter is released.

SEM micrographs of the surfaces of the calcined particles prepared with solutions A and B for 48 h of hydrothermal treatment at 100 °C are shown in Fig. 2. The surface of the spherical particles obtained employing solution A was composed of fine particles with a small number of aggregates exposed (Fig. 2a). The surface of the spherical particles obtained with solution B was less homogeneous and randomly

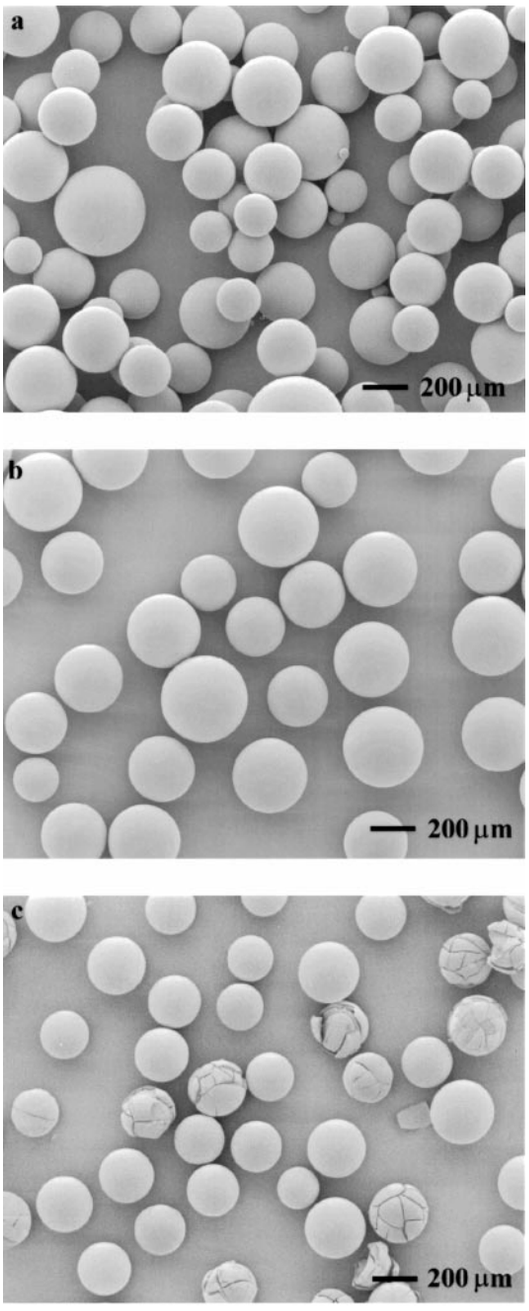

Fig. 1 SEM micrographs of (a) anion exchange resin beads, (b) resin–silicate composites synthesised with silicalite-1 synthesis solutions for 48 h of treatment at 100 °C and (c) the silicate particles obtained after the removal of the resin.

distributed crystals with a typical MFI morphology and a size of approximately 500 nm can be observed (Fig. 2b). The primary particles from the interior of the spheres were however similar to the ones shown in Fig. 2a for samples prepared from both solutions.

XRD analysis of the calcined materials obtained with solutions A and B showed that they were amorphous. To further investigate the short-range ordering of silica in the materials Raman spectroscopy was used. Raman spectra of the calcined products obtained with solutions A and B using the two types of resins are shown in Fig. 3. The spectra were baseline corrected and normalised to the intensity of the peak at 495 cm^{-1}. As seen from the figure there was no detectable difference in structure between: (i) the samples prepared with the two different types of gel resins, 1X2 and 2X8, and (ii) samples prepared with the two synthesis solutions, A and B. The Raman spectra presented are typical of amorphous

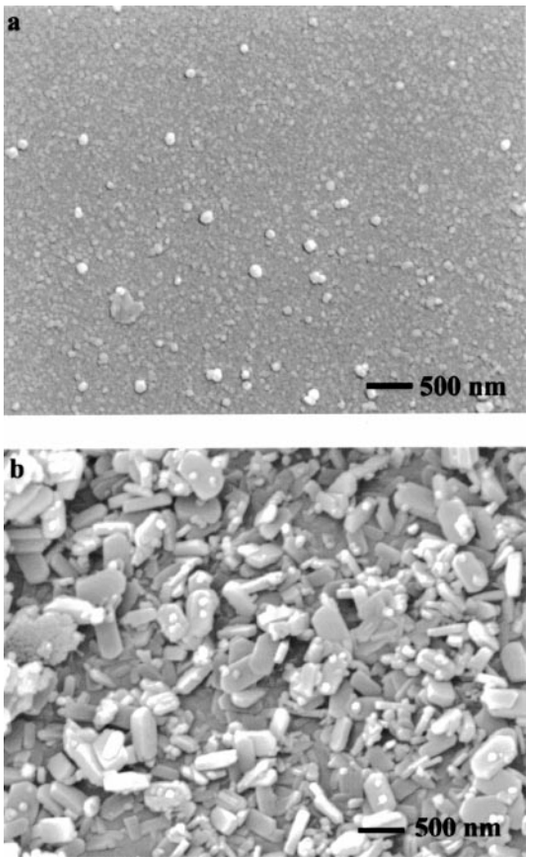

Fig. 2 The primary particles building up the surface of the calcined spherical particles prepared with solutions (a) A and (b) B.

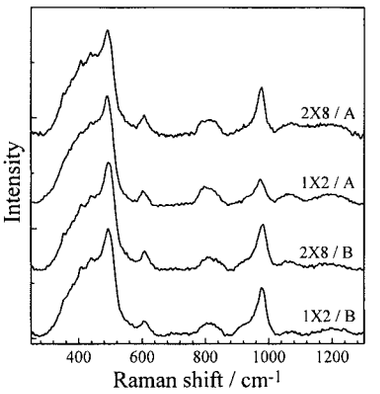

Fig. 3 Raman spectra of calcined spherical particles obtained after 48 h of treatment of the two types of resin at 100 °C with solutions A and B.

silica[17] and are discussed in detail elsewhere.[14] No peak at 380 cm^{-1}, the location of the most prominent peak in the Raman spectrum of silicalite-1, can be noticed in any of the Raman spectra indicating that silicalite-1 crystallisation takes place only in the bulk solution but not within the resin beads. This also shows that the number of the silicalite-1 crystals attached to the surface of the spherical particles obtained with solution B observed in the SEM images is small and therefore not detectable by Raman spectroscopy.

A comparison with the results obtained employing strongly basic styrene–divinylbenzene macroporous anion exchange resin where silicalite-1 crystallised in the pores of the resin[14] shows that the resin structure is crucial for the structure of the final products. Whereas macroporous resins contain distinct pores with a typical average pore diameter of about 150 nm and a pore size distribution ranging from several tens to several hundred nanometers, the gel resins are characterised by an "apparent porosity" of no greater than 4 nm which represents the average distance of separation of polymer chains.[18] Amorphous silica can readily be formed within the beads using both macroporous and strongly basic gel resins, whereas the further transition to an MFI structure cannot be realised within the gel resin beads, probably due to steric hindrance effects (*cf.* section 3.3).

A series of experiments was performed with solutions A and B diluted 10 and 20 times. The benefits from the dilution of the synthesis solutions are a shorter treatment time, a less complicated synthesis procedure and an easier separation of the resin–silicate composites from the mother liquid (since no silicalite-1 formed in the bulk).

The resin–silicate composites obtained with the diluted solutions were similar to the ones shown in Fig. 1b. SEM micrographs of the calcined materials obtained after the removal of the resin are shown in Fig. 4. The calcined particles synthesised using solution B10 were peeled off and shrunk

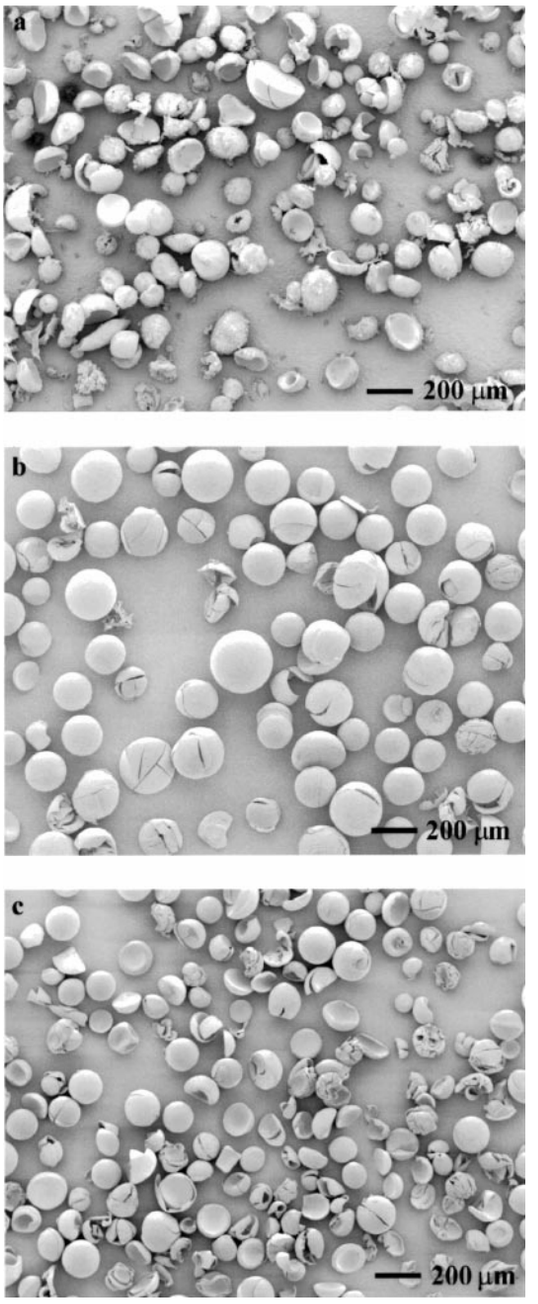

Fig. 4 SEM images of calcined particles obtained after 6 h of treatment at 100 °C with (a) B10, (b) A10 and (c) A20.

considerably upon calcination (Fig. 4a). The calcined particles obtained with solution A10 (Fig. 4b) were similar to the ones prepared with the non-diluted solution. However, when this solution was further diluted to 20 times and used in the same experiment, the resulting calcined particles also shrunk and partly peeled off (Fig. 4c).

The BET surface areas, total pore volumes as well as average pore diameters for the calcined materials obtained with the TPA–silicate solutions are listed in Table 1. The surface areas are all extremely high, for most samples exceeding 1000 $m^2\ g^{-1}$. From the results shown it can be concluded that: (i) the type of the initial resin does not considerably influence the BET surface area of the spherical particles obtained after the removal of the resin, (ii) slightly lower surface area values were obtained employing solution B and (iii) the dilution of solution A up to 20 times does not substantially affect the surface area of the materials obtained whereas the dilution of solution B 10 times results in a significant decrease of the BET surface area. Also, as seen from Table 1, larger pore volumes as well as larger average pore diameters were obtained for all materials prepared with the 2X8 resin in comparison with the ones for materials synthesised with the 1X2 resin.

Fig. 5 and 6 represent nitrogen adsorption isotherms for calcined materials obtained employing the two types of resins and solutions A and B. The inserts in each of the figures contain the corresponding BJH desorption ($dV/d\log(D)$) pore volume plots where D is the pore diameter. As seen from these figures different types of isotherms were obtained depending on the type of the initial ion exchange resin used. Fig. 5a illustrates the progressive reduction of pore sizes with an increase in concentration of solution A and using 1X2 resin as a macro-template. A transition from a type IV isotherm characteristic of mesoporous materials (A10 and A20) to a type I isotherm typical of microporous solids (solution A) is clearly seen.[19] The pore size distribution calculations confirm this reduction of pore size.

Different adsorption isotherms and relationships were obtained when the 2X8 resin was initially used (Fig. 5b). In this case mesopores were present in all materials as seen from the hysteresis loop in the isotherms and from the pore size distribution calculations. A possible reason for this difference in the pore structure between calcined materials prepared with the 1X2 and with the 2X8 resins is the different degree of cross-linkage of the two resins. The higher percentage of cross-linkage of the 2X8 resin is likely to result in a less homogeneous distribution of the silica species throughout the resin structure (*cf.* section 3.3). The difference is most pronounced when the undiluted solution A was used.

The adsorption isotherms for calcined samples obtained after treatment in solution B shown in Fig. 6 were all of type IV.

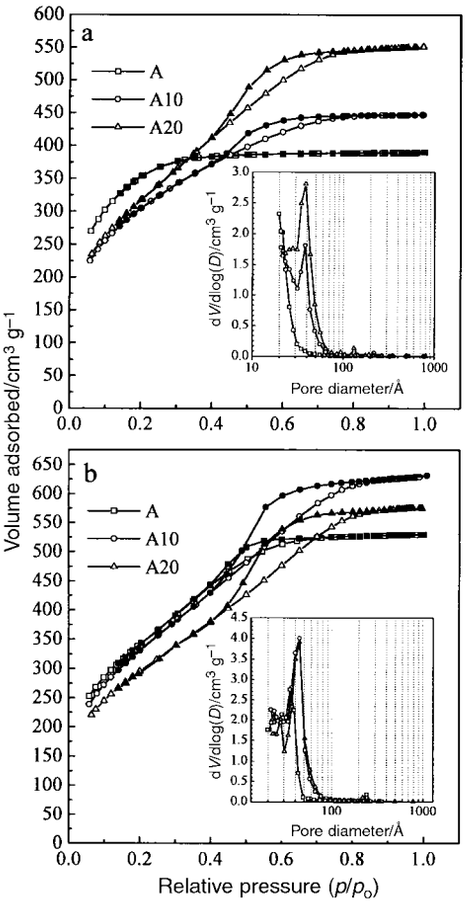

Fig. 5 Nitrogen adsorption isotherms at 77 K for samples prepared with solutions A, A10 and A20 using (a) 1X2 and (b) 2X8 resins. Open symbols, adsorption; solid symbols, desorption. The inserts represent the corresponding BJH desorption $dV/d\log(D)$ plots.

3.2 Sodium silicate solutions

Visually, the calcined materials obtained when the gel resins were treated with solution C (sodium silicate) at 100 °C for times between 6 and 50 h were similar to the materials prepared with the TPA–silicate solutions except for the fact that a substantial number of particles were black. The amount of black particles seemed to increase with an increase in the time of treatment and this amount was higher for particles prepared with the 1X2 resin in comparison with the 2X8 resin for equal times. The black particles appeared to be somewhat harder than the white ones. Entirely white particles were obtained with the 2X8 resin after 2 h of treatment in solution C at room

Table 1 BET surface area, total pore volume and average pore diameter for calcined materials obtained using different silica solutions

Resin type, solution, treatment time/h	BET surface area, $S_{BET}/m^2\ g^{-1}$	Total pore volume, $V_p/cm^3\ g^{-1}$	Average pore diameter, D^a/Å
1X2, A, 48 h	1278	0.60	18.8
1X2, A10, 6 h	1116	0.69	24.7
1X2, A20, 6 h	1169	0.85	29.1
2X8, A, 48 h	1248	0.82	26.3
2X8, A10, 6 h	1227	0.98	32.0
2X8, A20, 6 h	1089	0.89	32.7
1X2, B, 48 h	1028	0.74	28.8
1X2, B10, 6 h	852	0.69	32.7
2X8, B, 48 h	1081	0.90	33.3
2X8, B10, 6 h	751	0.84	44.7
1X2, C10, 6 h	1623	0.88	21.7
1X2, C20, 6 h	1390	0.83	23.9
2X8, C10, 6 h	1212	1.01	33.3
2X8, C20, 6 h	1224	0.89	29.1

[a]Calculated from the BET surface area and the total pore volume assuming cylindrical pores ($D = 4V_p/S_{BET}$).

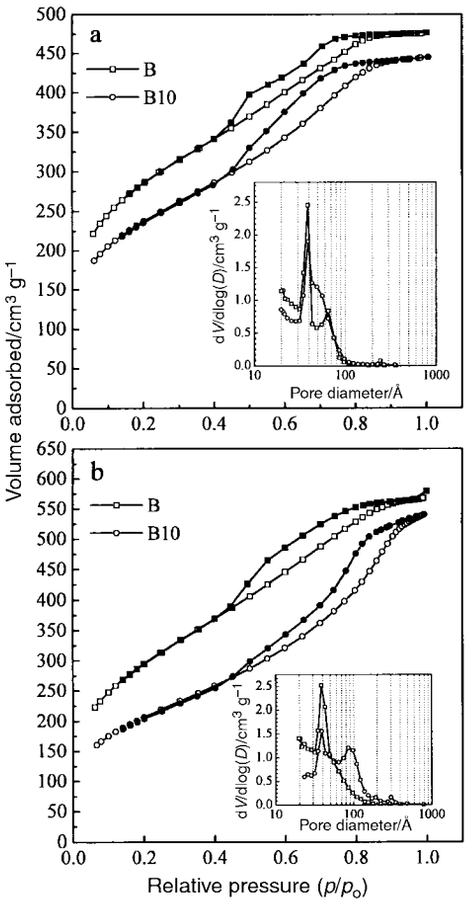

Fig. 6 Nitrogen adsorption isotherms at 77 K for samples prepared with solutions B and B10 using (a) 1X2 and (b) 2X8 resins. Open symbols, adsorption; solid symbols, desorption. The inserts represent the corresponding BJH desorption dV/d log(D) plots.

temperature. In the same experiment performed with the 1X2 resin some of the particles were black after calcination.

Micro-Raman (Renishaw 2000 using 780 nm laser line) spectroscopy was used to study the black particles obtained. In the Raman spectra of the black particles (not shown) peaks at about 1592 and 1320 cm^{-1} can be seen which reveal the presence of carbon phases.[20,21]

The BET surface areas of the calcined particles prepared at 100 °C using solution C were in the range 40–550 $m^2\ g^{-1}$ when the 1X2 resin was employed and in the range 350–580 $m^2\ g^{-1}$ for materials obtained with the 2X8 resin. The surface areas were decreasing whereas the number of black particles increased with increasing time of treatment. The surface areas obtained are substantially lower in comparison with the values for calcined materials prepared using solutions A and B. The decrease in the surface area is most probably due to the formation of carbon phases upon calcination when solution C was used. The higher surface area values for calcined macroparticles prepared with the 2X8 (yielding less black particles) resin confirm the later assumption.

In order to investigate whether sodium was present in the calcined particles synthesised using solution C, the SiO_2/Na_2O ratio was determined by ICP-AES in calcined samples prepared after treatment at 100 °C for 6 h with the two types of resin. The SiO_2/Na_2O ratios in these calcined samples obtained with the 1X2 and 2X8 resins were equal to 27.4 (74.0 wt% SiO_2, 2.7 wt% Na_2O) and 302 (95.5 wt% SiO_2, 0.316 wt% Na_2O), respectively. This result showed that sodium ions were generally rejected when the 2X8 resin was used. A greater amount of sodium was detected in the sample prepared with the 1X2 resin but the SiO_2/Na_2O ratio of this sample was still substantially higher than the ratio of the initial sodium silicate solution (3.19).

The rejection of sodium from the macroparticles is of interest from both fundamental and practical points of view. Fundamentally it shows that sodium is not strongly associated with the anionic silica species and consequently is not incorporated within the resin structure after the ion exchange process. For some practical applications, *e.g.* in catalysis, the presence of sodium is often undesirable due to deterioration of the thermal and hydrothermal stability of the materials.

Finally, experiments were performed with solutions C10 and C20 prepared by dilution of solution C. The calcined particles obtained after the treatment with the diluted solutions using both types of resin were similar to the ones prepared with the TPA–silicate solutions, *i.e.* no black particles were observed upon calcination. Fig. 7 shows SEM images of calcined particles obtained after treatment in solutions C10 (a) and C20 (b). These particles were shrunk in comparison with the corresponding resin–silicate composites and also the number of unbroken macroparticles seemed to be greater when C10 was

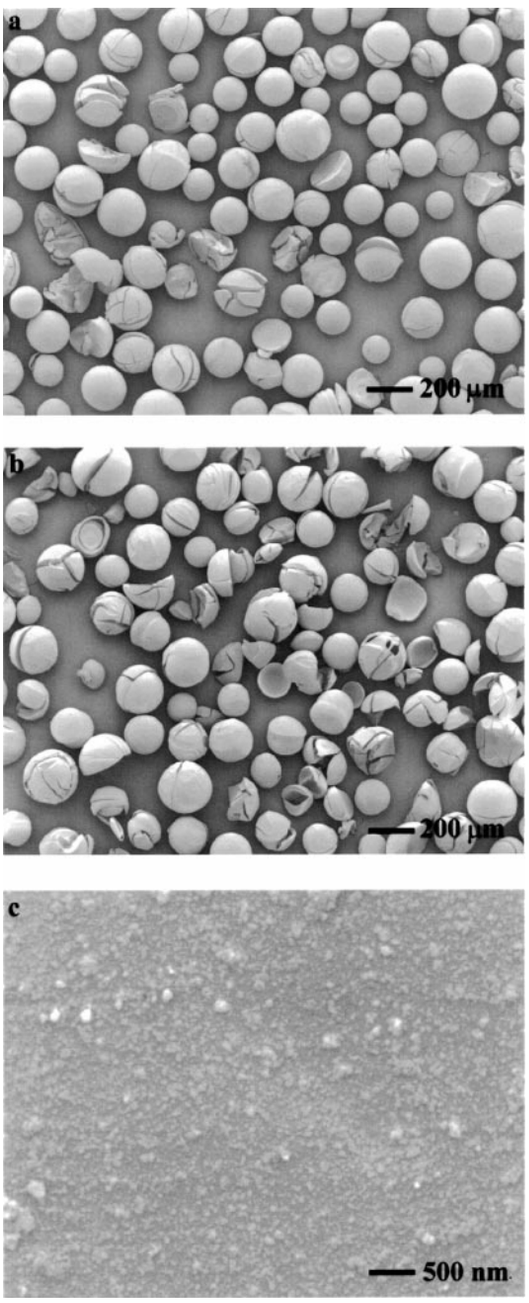

Fig. 7 SEM images of calcined macroparticles prepared using solution C10 (a), C20 (b) and the surface of the particles at high magnification (c).

used. The surface of the calcined particles (Fig. 7c) was very homogeneous and composed of fine particles.

BET surface areas, total pore volumes and average pore diameters for calcined materials prepared with the diluted solution C are listed in Table 1. Extremely high surface areas were obtained for calcined particles obtained when the 1X2 resin was treated with solutions C10 and C20. The high surface area values were confirmed by both repeated measurements and repeated experiments. Mesopores were present in all samples as seen from the nitrogen adsorption isotherms shown in Fig. 8 and from the calculated pore size distributions also presented in this figure. Similarly to the results for the TPA–silicate solutions, larger pore volumes and pore diameters were obtained when the 2X8 resin was initially used in the experiment with the diluted sodium silicate solutions.

3.3 Formation of the silica macroparticles

Although the exact mechanism for the formation of the macroparticles is not clear, a conceptual mechanism can be visualised. The first step of this mechanism most likely involves the introduction of silicate species into the resin by ion exchange. This step results in a composite material with a three-dimensional network of silica within the three-dimensional network of the polymer building up the resin. This composite material is then calcined in order to combust the organic anion exchange resin. A particle results with a shape and size similar to that of the original resin and with a porosity partly emanating from the removal of the organic fraction and partly due to the fact that the inorganic network remaining probably is built up of very small interconnected silica particles. It is well established that alkaline silicate solutions contain anionic silicate species present as monomers, oligomeric anions and subcolloidal particles possessing a negative surface charge.[22–24] The distribution of the silica between these different anionic species and the size of the subcolloidal silica particles are functions of a number of parameters including silica concentration, pH and the ageing time after preparation. To some extent the type of cation present may also influence the properties. Basically the fraction of silica present in more polymerised species (oligomers and particles) is higher the lower the pH (or the higher the molar ratio SiO_2/M_2O) is of the solution. Judging from literature data, the main part of the silica in solution A used in this study is likely to be found in colloidal silica particles with an average size of about 2 nm whereas this would also be true for solution B but with somewhat larger particles (about 3 nm). In solution C, a larger fraction (about 25%) of the silica is expected to be found in monomeric and oligomeric species and the particle size of the colloidal components should be between 1.5 and 2 nm. The effect of dilution of the alkali silicate on the average particle size of the colloidal species is complicated but it appears as if dilution to the extent used in the present study generally results in a slight increase of the average particle size. Since the surface area of the resulting material should be related to the size of the primary particles, these trends would indicate that solution B should yield the materials with the lowest surface area, solution A should give materials with an intermediate surface area and solution C should yield materials with the highest surface area. Judging from the data in Table 1, a general tendency in this direction does exist. A weakness of this line of argument is, however, that the size of the probe (nitrogen molecule, 0.35 nm) used for the surface area measurement is of the same order as the primary particles building up the material. This implies that the surface area as measured by nitrogen adsorption is a function not only of the size of these particles but also of their arrangement in the structure. A large fraction of the "surface area" may in reality not be accessible for the nitrogen molecules. Moreover, since the fraction of the surface area which is accessible for the nitrogen molecules is expected to be found in extremely small pores, the "multilayer" assumption used when applying the BET equation is most likely not fulfilled for a large fraction of the "surface area" of these materials.

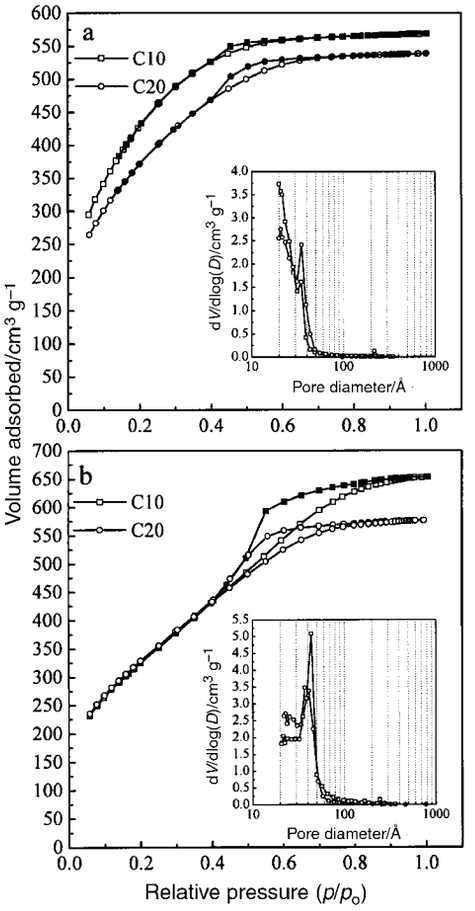

Fig. 8 Nitrogen adsorption isotherms at 77 K for samples prepared with solutions C10 and C20 using (a) 1X2 and (b) 2X8 resins. Open symbols, adsorption; solid symbols, desorption. The inserts represent the corresponding BJH desorption $dV/d\log(D)$ plots.

A factor making the analysis even more complicated is the fact that the behaviour of the gel type resins used in the study is sensitive to the chemical environment in the solution and presumably also to the size of the colloidal particles dominating the silicate solutions. The amount of silica as well as the size of the colloidal silica particles that can be introduced into the resin should to some extent be functions of the degree of swelling of the resin. This is particularly likely since the pore size of the gel resin is of the same order of magnitude as the size of the silicate species (around 4 nm). The swelling of gel type resins in general (i) increases with decreasing ionic strength of the solution (*i.e.* increasing dilution), (ii) decreases with increasing valency of the counter ion, and (iii) decreases with an increasing degree of cross-linking of the resin.[18] It is also known that specific interactions between the anionic species and the exchange sites of the resins can strongly influence the degree of swelling. It is at this point not known whether any such specific interactions are playing a role in the preparation of silica macrostructures. Since the silicate solutions do contain a variety of anionic species there will be competition between these species for the exchange sites of the resin. A general trend here is that species with a higher charge density are favoured from a selectivity point of view.[23] This obviously assumes that the exchange sites are not inaccessible for steric reasons. Considering the results achieved regarding the adsorption isotherms and the pore size distributions calculated from these isotherms for the various materials prepared in this study, it is possible to present explanations for the trends observed. Such

explanations would, however, be highly speculative. It appears reasonable, rather than presenting such explanations at the present time, to conclude that these systems are extremely complicated and that much more experimental work is needed in order to fully understand how various parameters affect their properties.

4 Conclusions

Spherical particles of amorphous silica were prepared by a procedure consisting of ion exchange of silica species into strongly basic gel resin beads followed by the removal of the resin by combustion. Large surface area materials (over 1000 $m^2 g^{-1}$) were prepared from TPA–silicate solutions containing tetraethoxysilane, tetrapropylammonium hydroxide and distilled water. Pore size distributions were dependent on the type of the initial resin used and the preparation of solely microporous materials and materials containing both micro- and mesopores was demonstrated. The pore size distribution was altered by diluting the starting synthesis solutions without substantially affecting the surface area values.

The type of starting resin appears to be crucial for the properties of the final product. Thus, when TPA–silicate solutions yielding silicalite-1 are used, two types of spherical particles may result depending on the initial resins employed: amorphous (using gel resins, the present paper) and crystalline (macroporous resins, ref. 14).

Spherical silica particles were also prepared employing gel type resins and commercial sodium water glass as a source of silica species. However, carbon phases were formed upon calcination of the resulting resin–silicate composites leading to a decrease in the surface area of the materials. Gel resins with higher cross-linkage were more stable towards the formation of carbon phases in these experiments. The problem of carbonisation can be overcome by diluting the initial sodium silicate solution. The BET surface areas of calcined materials obtained using diluted solutions were extremely high, up to 1600 $m^2 g^{-1}$.

Larger pore volumes and average pore diameters were obtained when a resin with higher cross-linkage was initially used for both TPA–silicate and sodium silicate solutions. Further research is required in order to evaluate the effects of various parameters on the properties of these materials.

The approach used to prepare the materials described may be useful for the preparation of other materials with shapes, sizes and porosity tuned prior to their application.

Acknowledgements

Financial support from the Swedish Research Council for Engineering Sciences (TFR) is gratefully acknowledged. The authors thank Dr. Boriana Mihailova for the Raman study of the materials described.

References

1 D. L. Wilcox Sr. and M. Berg, *Mater. Res. Soc. Symp. Proc.*, 1995, **372**, 4.
2 N. K. Raman, M. T. Anderson and C. J. Brinker, *Chem. Mater.*, 1996, **8**, 1862.
3 J. S. Beck, J. C. Vartuli, G. J. Kennedy, C. T. Kresge, W. J. Roth and S. E. Schramm, *Chem. Mater.*, 1994, **6**, 1816.
4 O. D. Velev, T. A. Jede, R. F. Lobo and A. M. Lenhoff, *Chem. Mater.*, 1998, **10**, 3597.
5 F. Caruso, R. A. Caruso and H. Möhwald, *Science*, 1998, **282**, 1111.
6 M. K. Titulaer, J. B. H. Jansen and J. W. Geus, *J. Non-Cryst. Solids*, 1994, **168**, 1.
7 H. Izutsu, F. Mizukami, P. K. Nair, Y. Kiyozumi and K. Maeda, *J. Mater. Chem.*, 1997, **7**(5), 767.
8 S. Schacht, Q. Huo, I. G. Voigt-Martin, G. D. Stucky and F. Schüth, *Science*, 1996, **273**, 768.
9 Q. Huo, J. Feng, F. Schüth and G. D. Stucky, *Chem. Mater.*, 1997, **9**, 14.
10 H. Yang, G. Vovk, N. Coombs, I. Sokolov and G. A. Ozin, *J. Mater. Chem.*, 1998, **8**(3), 743.
11 M. Grün, I. Laurer and K. K. Unger, *Adv. Mater.*, 1997, **9**, 254.
12 K. Schumacher, M. Grün and K. K. Unger, *Microporous Mesoporous Mater.*, 1999, **27**, 201.
13 W. Stöber, A. Fink and E. Bohn, *J. Colloid Interface Sci.*, 1968, **26**, 62.
14 L. Tosheva, V. Valtchev and J. Sterte, *Microporous Mesoporous Mater.*, 2000, **35–36**, 621.
15 D. C. Sherrington, *Chem. Commun.*, 1998, 2275.
16 A. E. Persson, B. J. Schoeman, J. Sterte and J. E. Otterstedt, *Zeolites*, 1994, **14**, 557.
17 D. W. Matson, S. K. Sharma and J. A. Philpotts, *J. Non-Cryst. Solids*, 1983, **58**, 323.
18 C. E. Harland, in *Ion Exchange: Theory and Practice*, The Royal Society of Chemistry, Cambridge, 1994, p. 46.
19 S. J. Gregg and K. S. W. Sing, in *Adsorption, Surface Area and Porosity*, Academic Press, 1982.
20 M. Nakamizo, R. Kammereck and P. L. Walker Jr., *Carbon*, 1974, **12**, 259.
21 M. J. Mattheews, M. A. Pimenta, G. Dresselhaus, M. S. Dresselhaus and M. Endo, *Phys. Rev. B*, 1999, **59**, R6585.
22 R. K. Iler, in *The Chemistry of Silica: Solubility, Polymerization, Colloid and Surface Properties, and Biochemistry*, John Wiley & Sons, New York, 1979.
23 C. J. Brinker and G. W. Scherer, in *Sol–Gel Science: The Physics and Chemistry of Sol–Gel Processing*, Academic Press, Boston, 1990.
24 J. E. A. Otterstedt, M. Ghuzel and J. Sterte, *J. Colloid Interface Sci.*, 1987, **115**, 95.